Nuclear Physics B295 [FS21] (1988) 443–463
North-Holland, Amsterdam

INTERACTING FERMIONS ON A RANDOM LATTICE

S.J. PERANTONIS and J.F. WHEATER

Department of Theoretical Physics, University of Oxford, 1 Keble Road, Oxford OX1 3NP, U.K.

Received 10 July 1987
(Revised 4 February 1988)

We extend previous work on the properties of the Dirac lagrangian on two-dimensional random lattices to the case where interaction terms are included. Although for free fermions the chiral symmetry of the doubles is spontaneously broken by their interaction with the lattice and they decouple from long-distance physics, our results in this paper show that all is undone by quantum corrections in an interacting field theory and that the end result is very similar to what is found with Wilson fermions. Two field-theoretical models with interacting fermions are studied by perturbation expansion in the field theory coupling constant. These are a model with one fermion and one boson species interacting via a scalar Yukawa coupling and the massive Thirring model. It is shown that on the random lattice ultraviolet finite diagrams and finite parts of ultraviolet divergent diagrams have the correct continuum limit. Ultraviolet divergent parts can be removed by the same renormalisation procedure as in the continuum, but do not exhibit the same dependence on the lagrangian mass. In the case of the massive Thirring model this causes a fermion mass correction of order the cut-off scale, which breaks the chiral symmetry of the remaining light fermion; there is consequently a fine-tuning problem. In the context of the same model we discuss the effect of the Goldstone boson associated with the spontaneous breakdown of the chiral symmetry of the doubles on two-dimensional models with vector couplings.

1. Introduction

Recently, the properties of fermions on random lattices have been extensively investigated, in particular at the tree graph level [1–4]. In ref. [1], it has been shown that the random lattice provides a natural way of (at least partially) alleviating the fermion doubling problem in two dimensions. Starting with a lattice version of the Dirac lagrangian which is chirally symmetric when the mass parameter $m \to 0$, it is found that the chiral symmetry of the double modes in the free fermion theory is broken. The doubles acquire large masses of the order of the inverse of the average lattice spacing a which do not vanish as $m \to 0$; they do not propagate further than a few lattice spacings on the random lattice, unlike the primaries which are insensitive to the randomness and have a mass equal to the lagrangian mass m. The fermion condensate $\langle \bar{\psi}\psi \rangle$ acquires a vacuum expectation value of order a^{-1}, and a study of the pseudoscalar Green function reveals a pole contribution of mass $\propto \sqrt{m/a}$ as well as that of the two primary fermion cut. The pole contribution is

0169-6823/88/$03.50

consistent with that expected from an approximate Goldstone boson associated with the spontaneous breakdown of the chiral symmetry of the doubles*. Thus, physics at distances of more than a few lattice spacings is described by an effective lagrangian containing a light fermion of mass m, some heavy fermions of mass $\sim a^{-1}$ and a pseudoscalar approximate Goldstone boson, which is a bound state of two doubles, of mass $m_G \sim \sqrt{m/a}$. The Goldstone boson couples to the fermions through a Yukawa interaction whose coupling strength was not determined in ref. [1] (we will determine it in this paper). In the continuum limit $a \to 0$ the Goldstone particle and the doubles become infinitely heavy (although the Goldstone is much lighter than the doubles) and only the contribution of the light fermion to Green functions survives; we therefore end up with a long-distance physics involving only a single species of light Dirac fermion. For further details we refer the reader to ref. [1].

In this paper we investigate what happens when interaction terms are added to the field theory lagrangian by considering the perturbation expansion in the field theory coupling constant. Our calculations are done using the exact free fermion propagators on the random lattice so that all the effects of randomness described in the previous paragraph are fully taken into account. As we will show, the doubles manifest themselves in the divergent parts of one-loop diagrams. We will also show that, if one regards the effects of doubling as described by the effective lagrangian discussed above, the contribution of the Goldstone boson in the finite parts of loop diagrams is readily detectable. This form of investigation does not of course reveal the full non-perturbative structure of the field theory lagrangian. However, experience shows that the problems of doubling always manifest themselves in a perturbation expansion in the field theory coupling constant (see for example the discussion of Wilson fermions in ref. [8]).

There are certain similarities between the picture briefly reviewed above, concerning the behaviour of fermions on the random lattice, and Wilson's method of evading the doubling problem on a regular lattice [7]. In this method the chiral symmetry of the double modes is explicitly broken by adding an appropriate term to the naive lattice action of the free fermion. The double modes acquire a mass of the order of the inverse lattice spacing and hence decouple from the theory in the continuum limit. Interacting fermionic field theories with Wilson fermions have been studied in weak coupling perturbation theory, mainly in the context of gauge theories [8, 9]. It is useful to bear in mind the main results of this work as an indication of what difficulties we might encounter when studying interacting ferm-

* What happens to the doubles is analogous to the situation in QCD where starting with a quark lagrangian mass m_q we find $\langle \bar{\psi}\psi \rangle \sim \Lambda^3$, a dynamical quark mass $m_{dyn}(p) \sim \Lambda^3/p^2$, and a pion mass $m_\pi \sim \sqrt{m_q/a}$. It might seem that the breaking of chiral symmetry is caused by the quenching procedure used to calculate Green functions. However, there would then be no Goldstone boson; as yet a complete analytical understanding of the mechanism is lacking.

ions on a random lattice. The value of primitively convergent diagrams consists of the relativistic contribution of each fermion (primary or double) and of other terms of the order of the lattice spacing. Insofar as the contribution of the doubles is suppressed because of the large mass they have acquired, the value of the diagram tends to the continuum result for the primary fermions. The same conclusion holds for the finite parts of the primitively divergent diagrams. The pole parts of these diagrams show the same structure as in the continuum limit, in the sense that they can be eliminated by the mass, wavefunction and coupling constant renormalisation. However, their dependence on the primary fermion mass is not the same as in the continuum theory. Their values are given by complicated integrals over the loop momenta and depend on the parameter r which determines the scale of the chiral-symmetry breaking.

One of the main objectives of any lattice model with fermions is ultimately to use it to study gauge field theories and in particular QCD. Given that our study of interacting fermionic field theories on the random lattice is going to be in two dimensions, a natural choice of an interacting field theory would be the two-dimensional abelian field theory – the Schwinger model. Although this model should be studied, it has the disadvantage – from our point of view – that it has no primitively divergent diagrams and hence does not fully serve our purpose of examining both finite and pole parts. We therefore turn to the study of a model with one fermion and one boson species interacting via a Yukawa coupling and of the massive Thirring model.

This paper is organised as follows. In sect. 2 we study the lowest order correction to the fermion and boson propagators in the Yukawa coupling model. In sects. 3 and 4 we study the one- and two-loop corrections to the fermion propagator in the massive Thirring model. Sect. 5 contains a discussion of our conclusions.

2. Fermion and boson with Yukawa interaction

The way in which our random lattice is constructed was first described in ref. [6]. A set of points with uniform distribution in a square is selected. If the circumscribed circle of any three points does not contain any other points, the three points are declared nearest neighbours and links are drawn joining them. In this way the whole plane is triangulated and there are no links crossing each other. The dual lattice is constructed by drawing the perpendicular bisectors of all the links. Periodic boundary conditions on all fields involved are used throughout this paper. We write the action of the model for a boson field Φ of mass m_b and a fermion field Ψ of mass m_f, interacting via a scalar Yukawa coupling on the random lattice, as follows

$$\mathcal{A}=\mathcal{A}_b+\mathcal{A}_f+g\sum_i \omega_i \Phi_i \bar{\Psi}_i \Psi_i . \tag{2.1}$$

$\mathscr{A}_b$ and $\mathscr{A}_f$ are the free boson and fermion actions [5,6]

$$\mathscr{A}_b = \tfrac{1}{4}\sum_{ij}\lambda_{ij}(\Phi_i - \Phi_j)^2 + \tfrac{1}{2}m_b^2\sum_i \omega_i \Phi_i^2, \tag{2.2}$$

$$\mathscr{A}_f = \tfrac{1}{2}\sum_{ij}\lambda_{ij} l_{ij}^{\mu}\bar{\Psi}_i\gamma_\mu\Psi_j + m_f\sum_i \omega_i\bar{\Psi}_i\Psi_i. \tag{2.3}$$

The Einstein summation convention is adopted for Greek indices only. Lattice sites are denoted by i, j, and γ_μ, $\mu = 1,2$, are the euclidean gamma matrices related to the x, y directions, respectively. The components of the vector linking the two end points of the link $\langle ij\rangle$ are denoted by l_{ij}^{μ}. The weight λ_{ij} is defined by

$$\lambda_{ij} = \begin{cases} \sigma_{ij}/l_{ij}, & \text{if } i, j \text{ are joined by a link} \\ 0, & \text{otherwise} \end{cases}. \tag{2.4}$$

Here l_{ij} is the length of the link $\langle ij\rangle$ and σ_{ij} is the length of the link on the dual lattice which intersects $\langle ij\rangle$. The area of the dual cell surrounding the point i is denoted ω_i. For simplicity (in order to keep a minimum number of parameters) we shall confine ourselves to the case $m_f = m_b = m$.

The diagrams which contribute to the lowest order correction to the fermion propagator are shown in fig. 1a. The first of these diagrams is ultraviolet finite in the continuum theory. We first examine the diagram with its external legs removed

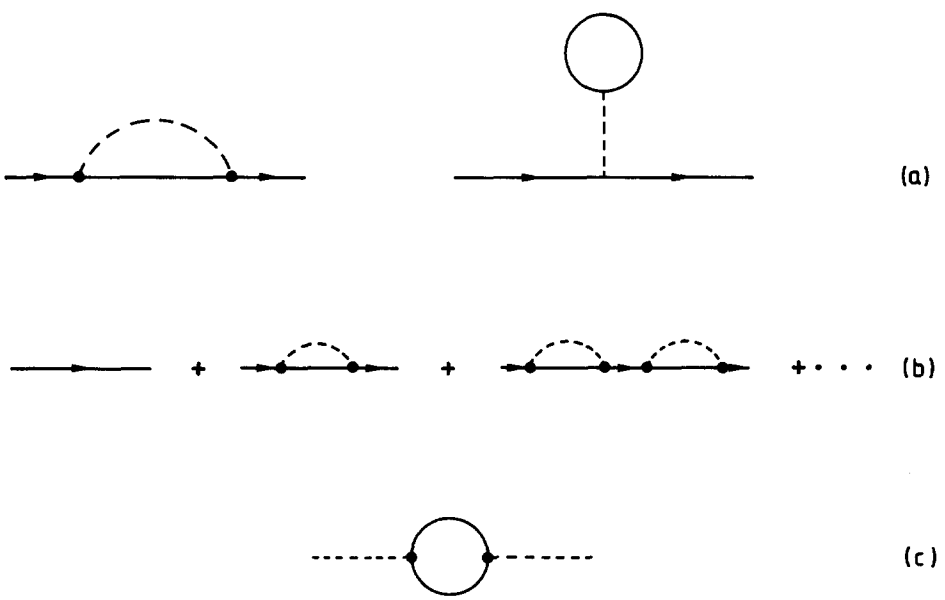

Fig. 1. Weak coupling perturbation-theory diagrams for the model of one fermion and one boson species interacting through a scalar Yukawa coupling. (a) Diagrams contributing to the lowest order correction to the fermion propagator. (b) Ultraviolet finite contribution to the full one-loop fermion propagator. (c) Lowest order correction to the boson propagator.

(the values of all diagrams with external legs removed will be presented in units of the coupling constant). We choose to study the "zero momentum" quantity $\Sigma_0(x)$ associated with this two-point function Σ which is defined in the continuum as

$$\Sigma_0(x) = \frac{1}{V}\int \mathrm{d}x'\,\mathrm{d}y'\,\mathrm{d}x''\,\mathrm{d}y''\,\Sigma(x'-x'', y'-y'')\,\delta(x-(x''-x')), \quad (2.5)$$

where V is the area of the box in which we enclose our system. In what follows all two-point functions will be zero momentum except where otherwise stated. On the random lattice the integral is replaced by a sum over the lattice sites i, j and the operator O_i is weighted by ω_i. Our results are presented averaged over bins of size $a/2$ in the x direction. In the continuum Σ_0 has the form

$$\Sigma_0^{\alpha\beta}(x) = f_1(x)\mathbf{1}^{\alpha\beta} + f_2(x)\gamma_1^{\alpha\beta}, \quad (2.6)$$

with $f_1(x) = f_1(-x)$ and $f_2(x) = -f_2(-x)$. We have checked that on the random lattice the coefficients of the matrices γ_2 and γ_5 are small and oscillate around the value 0. Fig. 2 shows Σ_0^{11} computed on a random lattice with 900 sites. In the same figure the corresponding continuum result calculated in a box of the same size is

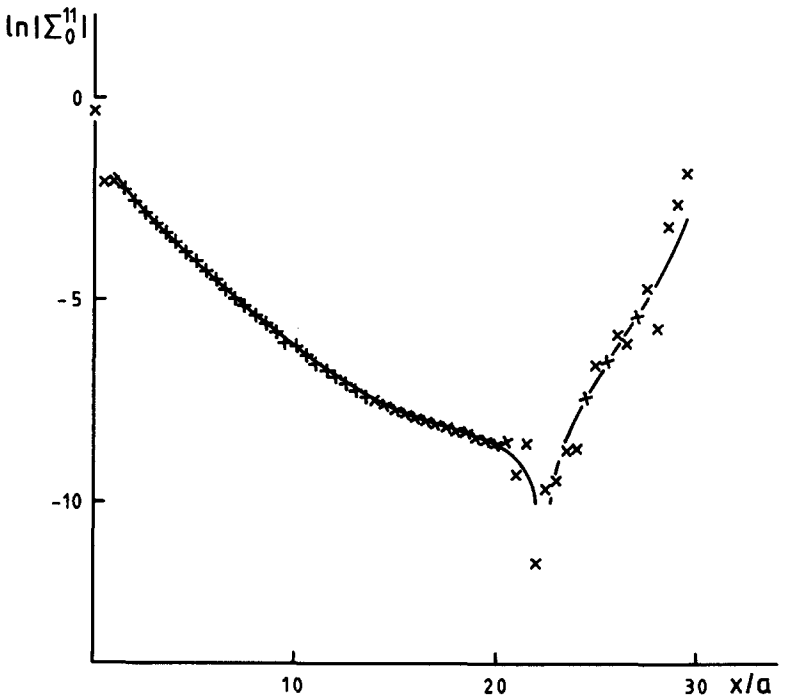

Fig. 2. A logarithmic plot of our random lattice measurements for the first diagram of fig. 1a with the external legs removed. A 900-site lattice and a value of $ma = 0.20$ have been used. The solid curve shows the corresponding continuum result calculated in a box the same size as our random lattice. Σ_0^{11} changes sign near $x/a = 22$.

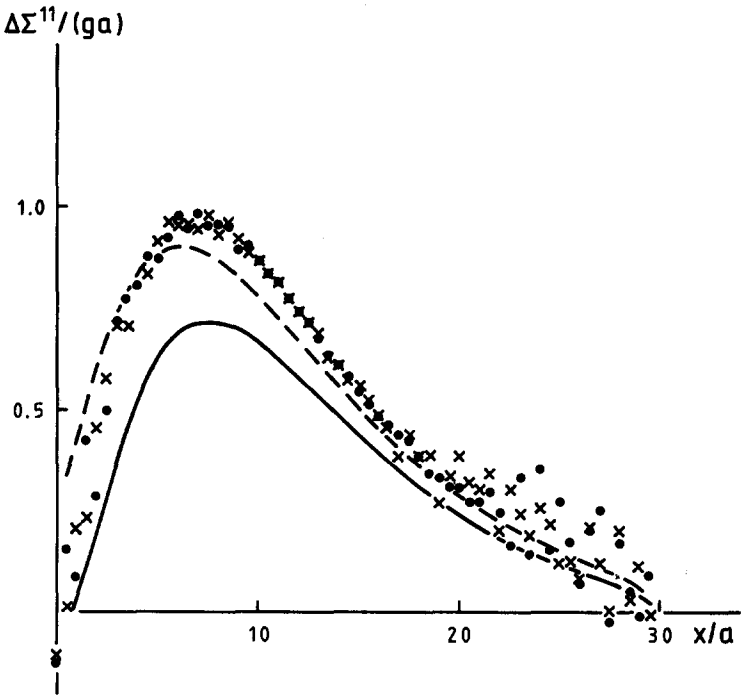

Fig. 3. The ultraviolet finite contribution to the full one-loop correction to the fermion propagator in the Yukawa coupling model divided by the square of the coupling constant g. Data from two 900-site random lattices are shown for $ma = 0.20$ and $ga = 0.1$. The solid curve represents the continuum result. The dashed curve is obtained with Wilson fermions on a 900-site regular square lattice and with $r = 1$.

shown. The random lattice result closely resembles the continuum curve for all values of x except for very small distances.

To check that the first diagram of fig. 1a has the expected behaviour in the continuum limit, we must attach the external legs. This is because the bad short-distance behaviour of the tree-level fermion propagator may affect the one-loop fermion propagator; on summing over the interaction points we encounter distances between the interaction and the external points which are arbitrarily short. We have thus examined the full connected fermion propagator including all the ultraviolet finite one-loop effects (fig. 1b) in position space. In fig. 3 we show the quantity $\Delta\Sigma^{11}/(ga)^2$ where $\Delta\Sigma$ is the difference of the corrected and the tree-level fermion propagator as a function of x/a. Results from two different 900-site lattices are presented for the same value of ma and ga. In the same figure we show the corresponding continuum curve and the curve obtained with Wilson fermions on a regular square lattice the same size as our random lattice and with the Wilson parameter r equal to 1. The continuum and random lattice curves have the same shape and almost the same normalisation. In fig. 4 the relative difference, $(\Delta\Sigma^{11}_{\ell} -$

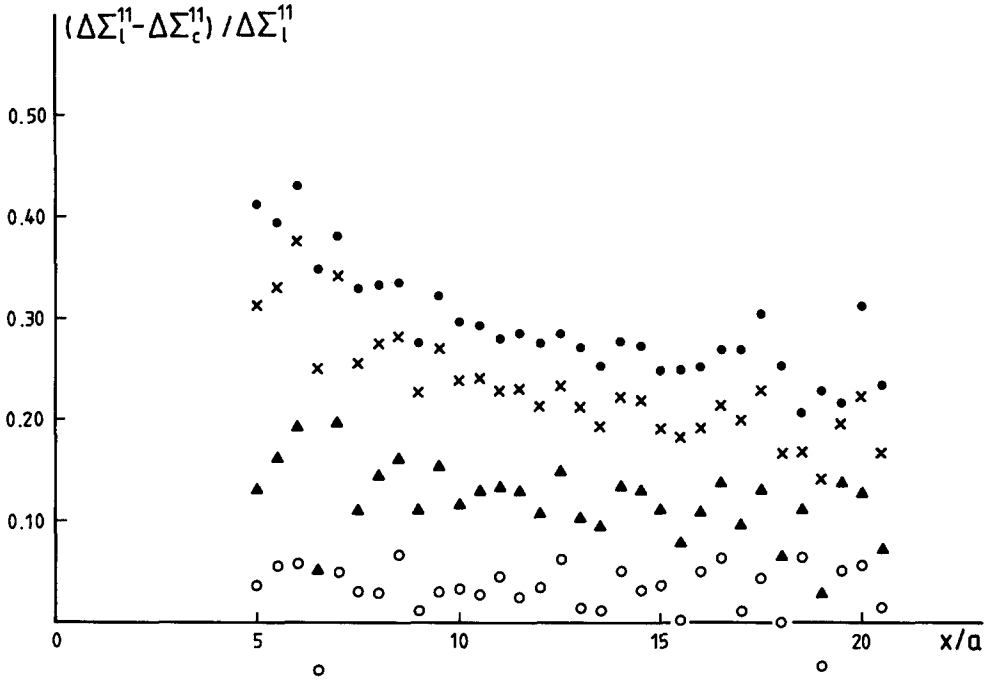

Fig. 4. The ratio $(\Delta\Sigma_\ell^{11} - \Delta\Sigma_c^{11})/\Delta\Sigma_c^{11}$ as a function of the lattice distance x/a for different values of ma. Here, $\Delta\Sigma_\ell$ is the ultraviolet finite contribution to the full one-loop correction to the fermion propagator in the Yukawa coupling model as calculated on the random lattice and $\Delta\Sigma_c$ is the corresponding continuum quantity. The data are from a 900-site random lattice with a small value of the coupling constant. ● corresponds to $ma = 0.20$. × corresponds to $ma = 0.15$. ▲ corresponds to $ma = 0.10$. Finally, ○ corresponds to $ma = 0.06$.

$\Delta\Sigma_c^{11})/\Delta\Sigma_c^{11}$, is plotted against x/a for different values of ma (the subscripts ℓ, c meaning "lattice" and "continuum", respectively). This ratio decreases as we approach the continuum limit $ma \to 0$ showing that $\Delta\Sigma_\ell^{11}$ approaches the continuum curve with decreasing ma. An interesting feature of the random lattice data in fig. 3 is that there is very little difference between the results of different random lattices with the same number of points, at least for distances which are large in comparison with the average lattice spacing. Hence, a systematic averaging over a large number of random lattices is not necessary. We will see that this is not always the case with ultraviolet divergent diagrams.

The second diagram of fig. 1a (tadpole diagram) is logarithmically divergent in the continuum. The fermion loop gives a contribution proportional to the fermion condensate $\langle\bar{\Psi}\Psi\rangle$ of the tree-level theory. Because of the spontaneous breakdown of the chiral symmetry on the random lattice, the fermion condensate acquires a value of order $1/a$. Hence, the continuum limit of this diagram calculated on the random lattice cannot be the same as the corresponding continuum diagram which

behaves like $m \ln m$. The resulting fine-tuning problem is similar to that arising in the Thirring model which is discussed in detail in sect. 3.

The lowest order correction to the boson propagator is given by fig. 1c. We have studied this diagram with the external legs removed, but we have checked on small lattices that the inclusion of external legs does not significantly alter the results. Let us call $G_b(p)$ the Fourier transform of this diagram. In order to produce $G_b(p)$ on the random lattice, we first calculate the diagram in position space and then Fourier transform the result. This diagram is in fact proportional to the "scalar meson" propagator in the free fermion theory, which has been studied in ref. [1] in position space and has been found to be in very good agreement with the continuum in all but the shortest distances. In the infinite-volume continuum theory $G_b(p)$ exhibits a logarithmically divergent correction to the boson mass. In studying the diagram on the random lattice, we are interested separately in the finite and in the pole part. We thus first study the momentum-dependent part – which is finite –

$$G_b(p) - G_b(p=0),$$

as a function of the lattice momentum for different values of the lagrangian mass

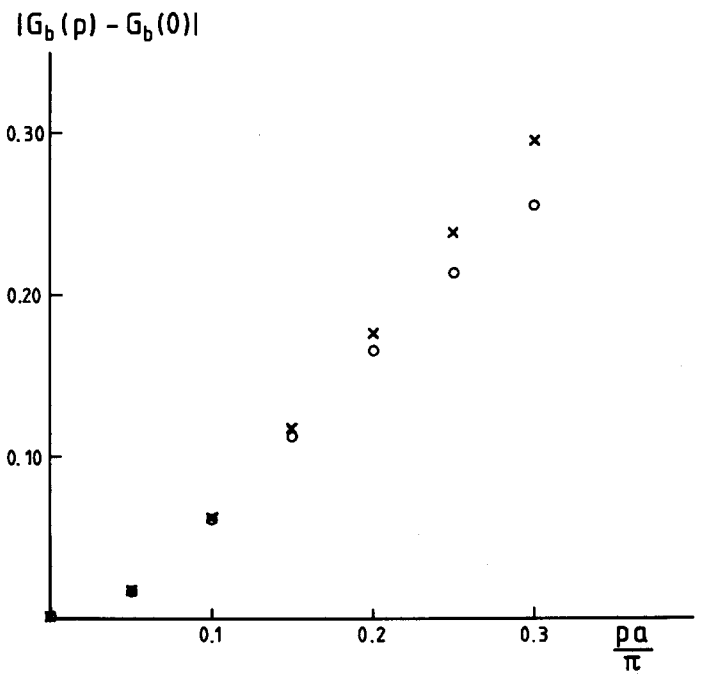

Fig. 5. The momentum-dependent part, $G_b(p) - G_b(p=0)$, of the lowest order correction to the boson propagator in the Yukawa coupling model in momentum space and with the external legs removed. × is the random lattice result obtained from a 1600-site random lattice with $ma = 0.18$. ○ is the corresponding continuum result calculated in a square box the same size as our random lattice. The two results are in very good agreement with each other for small values of the lattice momentum.

$m = m_f = m_b$. Results from a particular 1600-site lattice are presented in fig. 5 along with the corresponding continuum values calculated in a rectangular box the same size as our random lattice. These results are in very good agreement for small values of the momentum. The divergent part of the diagram is contained in $G_b(0)$. In the infinite-volume continuum theory

$$G_b(p=0) = \frac{1}{\pi}\ln\left(\frac{m}{\Lambda}\right) - \frac{1}{\pi} + \text{constant}, \tag{2.7}$$

where Λ is the ultraviolet momentum cutoff and the additive constant depends on the method of regularisation (in the case of a cutoff with the same value in all directions it is equal to zero). In a finite-volume system, the logarithmic behaviour can be hidden for sufficiently small ma because of finite-size effects. Fig. 6 shows the random lattice result obtained on a 900-site lattice and the continuum result in a rectangular box the same size as our random lattice with a momentum cutoff corresponding to a regular square lattice. There seems to be no agreement between the random lattice and the continuum result. It would be interesting to analyse $G_b(0)$ using finite-size scaling methods to extract the infinite-volume limit. Unfor-

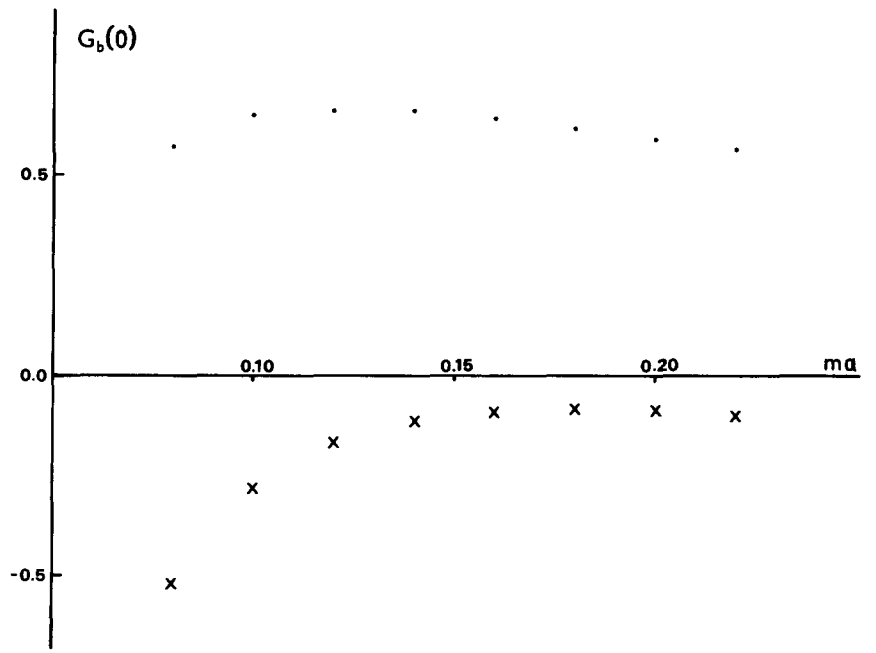

Fig. 6. The momentum-independent part, $G_b(p=0)$, of the lowest order correction to the boson propagator (with the external legs removed) for different values of ma. × are random lattice data obtained from a 900-site lattice. ● are the corresponding continuum data calculated in a square box the same size as our random lattice.

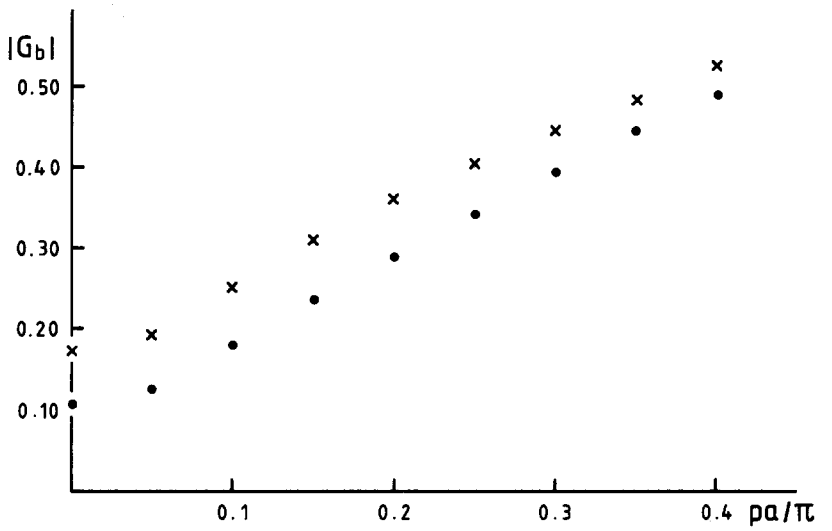

Fig. 7. $G_b(p)$ as a function of the lattice momentum on two different 1600-site random lattices.

tunately, it shows considerable fluctuation from random lattice to random lattice. Fig. 7 shows G_b as a function of the lattice momentum for two random lattices of 1600 sites each. Although the two curves are parallel, at least for relatively small values of the lattice momentum, there is a significant difference between the values of their momentum-independent parts. It is evident that the short-distance structure of a particular finite-size random lattice affects the ultraviolet divergent part of the diagram. This cannot be true in the infinite-volume limit, but we have witnessed no discernible trend towards the expected infinite-volume behaviour on lattices of up to 1600 sites.

If a pseudoscalar Yukawa interaction $g\sum_i \Phi_i \overline{\Psi}_i \gamma_5 \Psi_i$ is used in eq. (2.1), the tadpole correction to the fermion propagator vanishes; the full one-loop fermion propagator on the random lattice takes the continuum value in the limit $ma \to 0$. However, the boson self-energy receives contributions from the Goldstone and so does not exhibit the ultraviolet behaviour of the corresponding diagram in the continuum theory.

3. Massive Thirring model: one-loop diagram

In a euclidean continuum space the massive Thirring model has action

$$\mathscr{A}_T = \mathscr{A}_f - g\sum_i \int d^2x j_\mu(x) j_\mu(x), \tag{3.1}$$

where j_μ, $\mu = 1,2$ are the components of the current

$$j_\mu(x) = \overline{\Psi}(x)\gamma_\mu \Psi(x). \tag{3.2}$$

In the continuum theory the components of the current j have to be defined as the local limits of non-local products of operators [10]. On the random lattice there are several ways in which to define the interaction term. We will consider the three most local forms of the interaction term in the action

$$\mathscr{A}_{\mathrm{I},\alpha} = -\left(\tfrac{1}{4}\alpha\right)\sum_{ij}\left(\overline{\Psi}_i\gamma_\mu\Psi_j\right)\left(\overline{\Psi}_j\gamma_\mu\Psi_i\right)\sigma_{ij}l_{ij}, \tag{3.3a}$$

$$\mathscr{A}_{\mathrm{I},\beta} = -\left(\tfrac{1}{4}\beta\right)\sum_{ij}\left(\overline{\Psi}_i\gamma_\mu\Psi_j\right)\left(\overline{\Psi}_i\gamma_\mu\Psi_j\right)\sigma_{ij}l_{ij}, \tag{3.3b}$$

$$\mathscr{A}_{\mathrm{I},\gamma} = -\gamma\sum_{i}\left(\overline{\Psi}_i\gamma_\mu\Psi_i\right)\left(\overline{\Psi}_i\gamma_\mu\Psi_i\right)\omega_i. \tag{3.3c}$$

Each of these expressions has the interaction term in eq. (3.1) as its naive continuum limit (with g equal to α, β and γ respectively). The first two definitions are more natural in the sense that j is a vector current, normally associated with a link on the lattice. Of course, any linear combination of $\mathscr{A}_{\mathrm{I},\alpha}$, $\mathscr{A}_{\mathrm{I},\beta}$, $\mathscr{A}_{\mathrm{I},\gamma}$ may also be used. The lowest order correction to the fermion propagator is shown in fig. 8a. In the continuum theory and in momentum space this diagram (with the external legs removed) is momentum independent and leads to a mass shift

$$\Delta m = -\frac{2gm_{\mathrm{f}}}{\pi}\ln\left(\frac{m_{\mathrm{f}}}{\Lambda}\right), \tag{3.4}$$

where Λ is a momentum cutoff. The full fermion propagator including all one-loop effects (fig. 8b) is a linear combination of the unit matrix and γ_1 only. The sum S_{F} of the coefficients of these matrices shows, in a square box of side L, an exponential

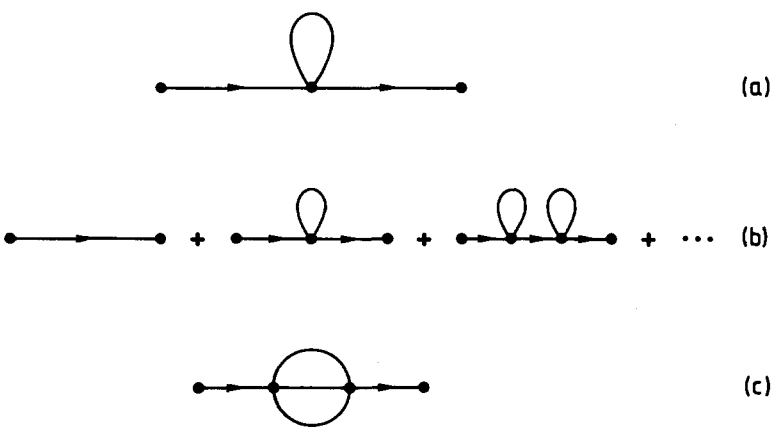

Fig. 8. Weak coupling perturbation-theory diagrams for the massive Thirring model. (a) Lowest order correction to the fermion propagator. (b) Full one-loop fermion propagator. (c) Second-order correction to the fermion propagator.

dependence on the coordinate x

$$S_F = \frac{e^{-(m_f+\Delta m)x}}{1-e^{-(m_f+\Delta m)L}}, \qquad 0 < x < L. \tag{3.5}$$

The fact that the lowest order correction to the fermion propagator is momentum independent makes this diagram a good candidate for studying the properties of divergent diagrams on the random lattice. We want to check the structure of S_F to discover if it has the correct exponential dependence on x. Provided the correct structure emerges, we wish to study the dependence of the radiative mass correction on m_f. Fig. 9 shows the results for S_F as a function of x calculated on a 400-site random lattice for various values of the lattice mass $m_f a$. The data are very well fitted by exponential curves except at very small distances. This is true for all three definitions of the interaction (eq. (3.3)). The normalisation of these exponentials is

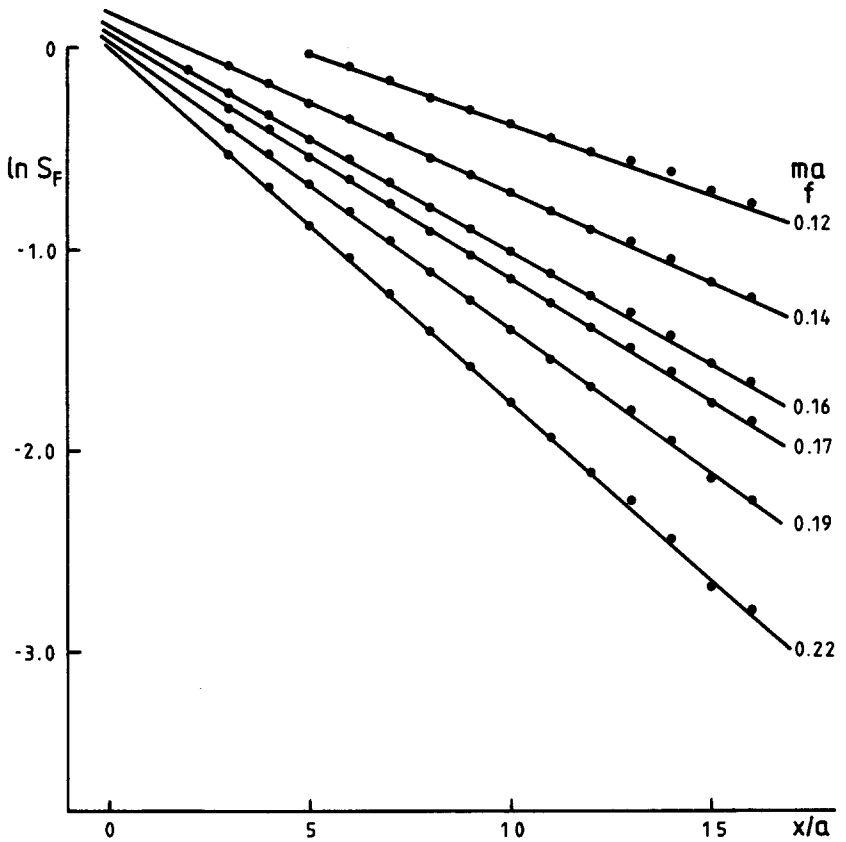

Fig. 9. The full one-loop fermion propagator in the massive Thirring model calculated on a 400-site random lattice in position space for various values of the tree-level mass $m_f a$. The interaction is defined as in eq. (3.3b) and the coupling constant is $\beta = 0.1$.

close to 1. The small deviation from this value, which grows with decreasing $m_f a$, is, within the errors induced by the smallness of our lattice, consistently explained as the result of finite-size effects. We conclude that S_F has the same structure on the random lattice as in the continuum, with the one-loop effects resulting in a mass renormalisation, no positive evidence having arisen for any additional effect (e.g. wave function renormalisation).

In the continuum the mass correction Δm vanishes as $m_f \to 0$. In a lattice formulation of the theory, it is desirable that the lattice radiative mass correction $a\Delta m$ retains the property $a\Delta m \to 0$ as $am_f \to 0$. In this case, the continuum limit, where the renormalised mass m_R times the lattice spacing goes to zero, coincides with the limit where am_f goes to zero, and hence can be approached with ease. This situation is in contrast with the case where the radiative mass correction contains terms proportional to the inverse lattice spacing and refuses to vanish as we take the limit $am_f \to 0$. In this case, approaching the continuum limit is more tedious; a mass renormalisation counterterm has to be introduced and adjusted (fine tuned) at each order of perturbation theory, so that the resulting m_R has no part proportional to $1/a$. Fig. 10 shows the value of $a\Delta m/g$ for different values of $m_f a$ and for the

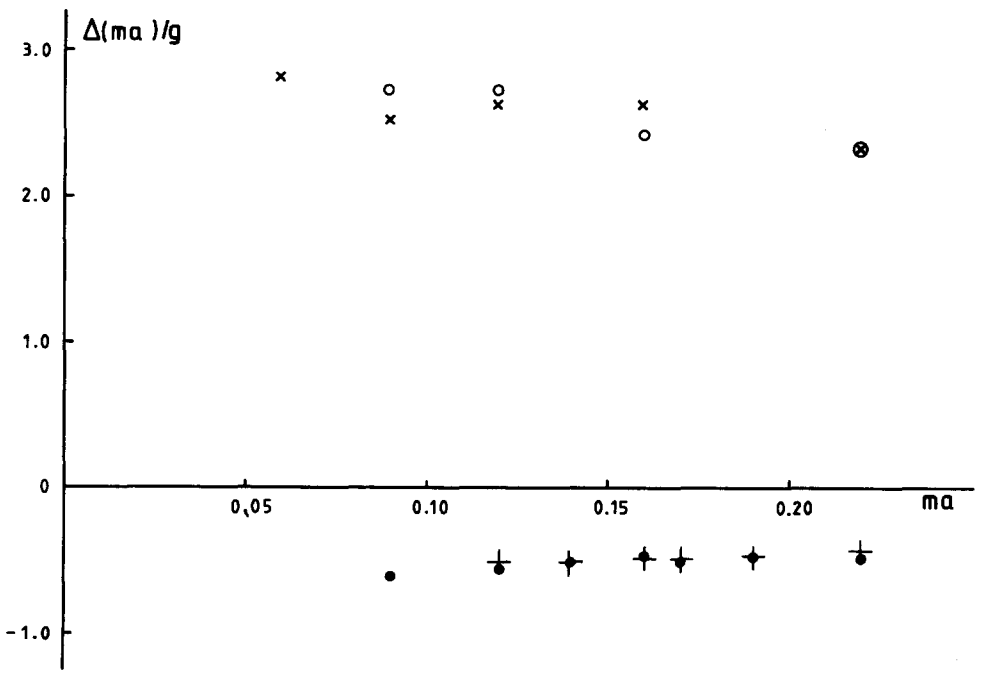

Fig. 10. The one-loop radiative correction to the fermion mass in the massive Thirring model (in units of the coupling constant) as a function of $m_f a$. The results are from a 400-site lattice and for various definitions of the Thirring interaction as discussed in the text. × corresponds to $\alpha = 0.01$. ● and + correspond to $\beta = 0.05$ and $\beta = 0.1$. ○ corresponds to $\gamma = 0.01$.

different definitions of the Thirring interaction, as calculated from exponential curves like those in fig. 9. In all cases we have also calculated $\Delta m/g$ by studying the diagram of fig. 8a with its external legs removed on the random lattice, and we have found that the values of $\Delta m/g$ obtained from the two procedures are in good agreement with each other. It is evident that $a\Delta m/g$ approaches a non-zero value as $m_f a$ decreases approaching zero. Hence, although the diagram under consideration has the correct structure and the part which diverges as the momentum cutoff tends to infinity can be removed by renormalising the mass, there is a fine-tuning problem. The fluctuation of the results corresponding to different random lattices of finite size renders this fine-tuning problem, from a practical point of view, probably more worrying than the corresponding problem with Wilson fermions. The bad behaviour of the one-loop fermion self energy is, of course, the result of the spontaneous breakdown of the chiral symmetry of the massless Dirac operator on the random lattice. Indeed, the non-vanishing part of the diagram of fig. 8a, with its external legs removed, is proportional to the quantities

$$(1/V)\sum_i \mathrm{Tr}(F_{jj})\omega_i, \qquad (1/4V)\sum_i \mathrm{Tr}(F_{ji})\,\sigma_{ij}l_{ij}, \qquad (1/V)\sum_i \mathrm{Tr}(F_{ii})\omega_i,$$

respectively, for each of the three definitions of the interaction in eq. (3.3). Here, F_{ij} is the tree-level fermion propagator from point j to point i which in these formulae are nearest neighbours, V is the total area of the random lattice and the trace is taken over spinor indices. Each of the expressions corresponds to a different definition of the tree-level fermion condensate $\langle\bar{\Psi}\Psi\rangle$ on the random lattice. The non-vanishing of the fermion condensate in the limit $am_f \to 0$ is the signal for spontaneous chiral-symmetry breakdown. The negative values of $\Delta m/g$ when eq. (3.3b) is used to define the interaction arise because the trace of the tree-level fermion propagator is negative at short non-zero distances, as shown in fig. 2b of ref. [4].

4. Massive Thirring model: two-loop diagram

In the continuum and in momentum space, the second-order correction to the fermion propagator (fig. 8c) exhibits an ultraviolet logarithmic divergence proportional to $p_\mu\gamma_\mu$. Here, we will not examine the ultraviolet divergent part of the diagram. However, we will show how the approximate Nambu–Goldstone boson associated with the spontaneous breaking of the chiral symmetry contributes to a non-trivial diagram, by examining the trace of the two loop diagram.

According to Goldstone's theorem, the spontaneous breakdown of the chiral symmetry of the double modes on the random lattice results in the emergence of a pseudoscalar boson, which is massless in the absence of a fermion mass term. When, however, $m_f \neq 0$, the chiral symmetry is also explicitly broken and it has been argued [1] that the situation in the doubled sector is similar to the PCAC picture of QCD. Since chiral symmetry breaks with a fermion condensate of order $1/a$, PCAC

and current algebra predict for the mass of the Goldstone

$$m_G^2 \sim m_f \langle \bar{\Psi}\Psi \rangle \Rightarrow m_G \sim \sqrt{m_f/a}\,. \tag{4.1}$$

The Goldstone is assumed to couple to the primary fermions via an effective pseudoscalar Yukawa coupling

$$f_G \bar{\Psi}\gamma_5 \Psi \varphi\,,$$

where φ is the Goldstone field. The validity of the whole picture can be checked by studying the pseudoscalar sector of the theory at the tree level. The correlation function between pseudoscalar operators $\bar{\Psi}_i\gamma_5\Psi_i$ sitting on different points of the random lattice should be affected by the presence of the Goldstone, its value being equal to the sum of a contribution coming from the primary fermions and a

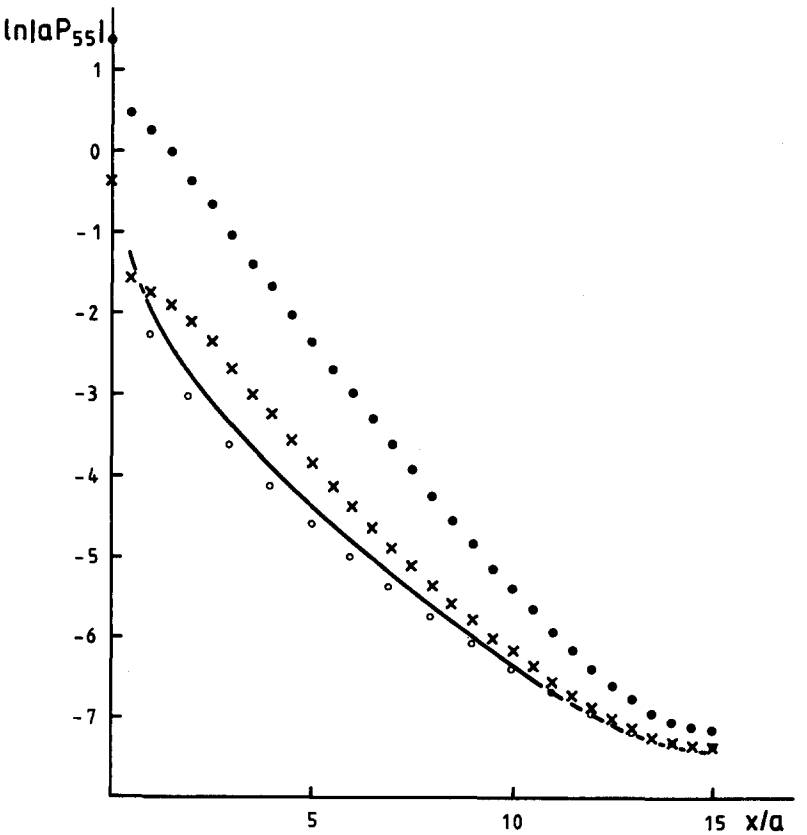

Fig. 11. Correlation functions for different pseudoscalar operators. ● is the point–point and × is the bond–bond correlation function. The data are from a 900-site lattice with $m_f a = 0.16$. The solid curve represents the continuum result. ○ is the point–point correlation function calculated with Wilson fermions on a 900-site regular square lattice and with the Wilson parameter r equal to 1.

contribution coming from the Goldstone. As discussed in ref. [1], the Goldstone contribution can be separated by considering the correlation function between point-split (or bond) pseudoscalar operators $\frac{1}{2}(\bar{\Psi}_i\gamma_5\Psi_j + \bar{\Psi}_j\gamma_5\Psi_i)$, where i and j are nearest neighbours. This correlation function is not expected to be significantly affected by the Goldstone if the size of its wave function is of the order of the lattice spacing. In fig. 11 we show the correlation function for the two types of pseudoscalar operator. Their difference δ is expected to be proportional to the propagator for the Goldstone

$$\delta = \frac{f_G^2}{2m_G} \frac{\cosh[m_G(L/2 - x)]}{\sinh(m_G L/2)}. \tag{4.2}$$

The data for this difference are very well fitted by a hyperbolic cosine (fig. 12)

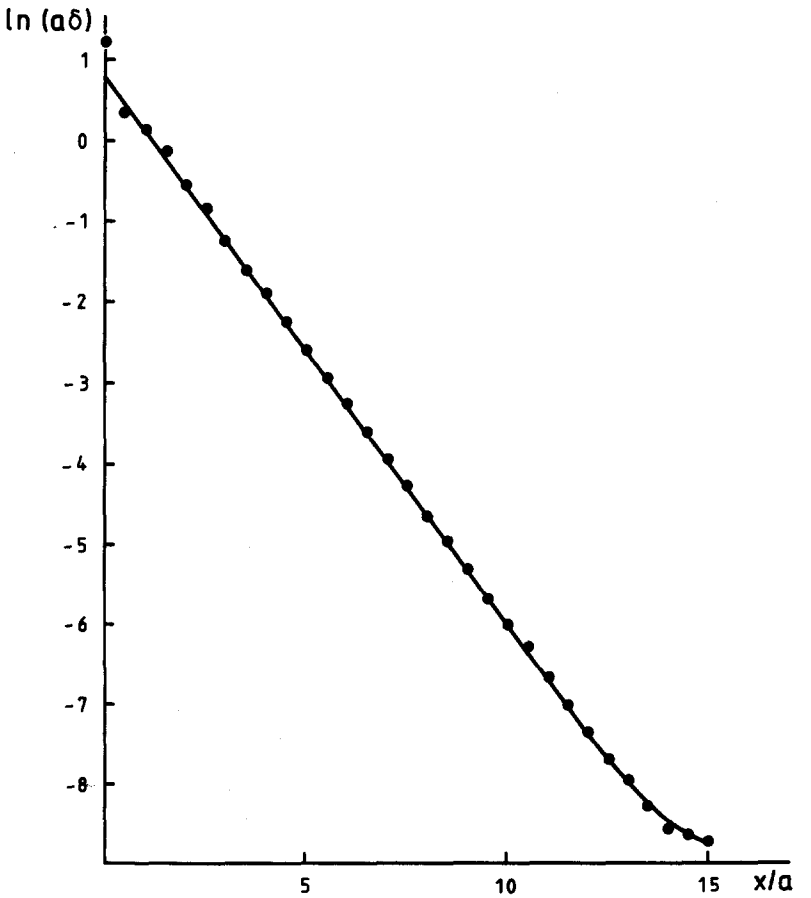

Fig. 12. A logarithmic plot of the difference of the two correlation functions of fig. 11 as a function of the distance on the random lattice. The curve is very well fitted by a hyperbolic cosine.

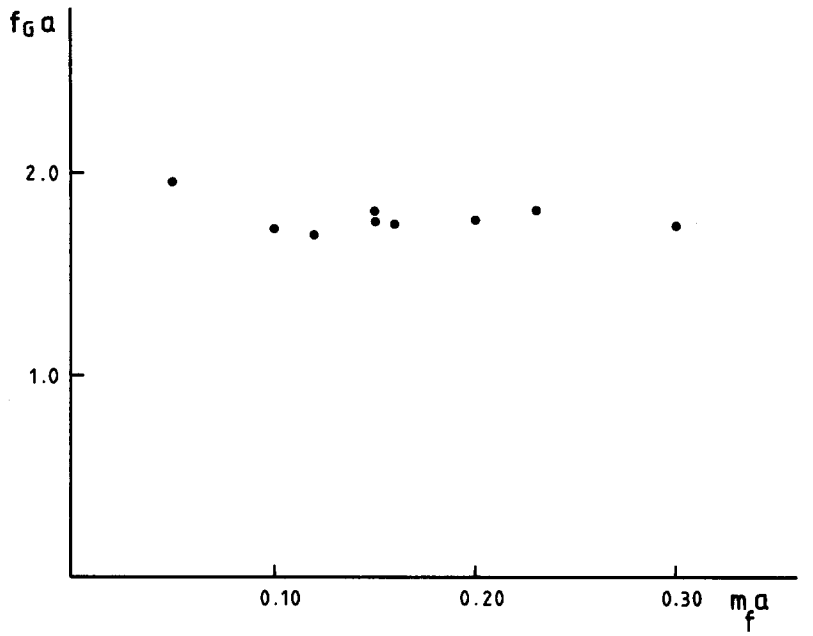

Fig. 13. The coupling f_G of the Goldstone boson to the primary fermions. The data are from different random lattices and for various values of $m_f a$. In all cases we obtain a value ≈ 1.7.

enabling us to extract the values of m_G and f_G (in this case, $m_G = 0.68$ and $f_G = 1.74$). By determining these quantities for different values of m_f and for different random lattices we can check the validity of the whole picture. The approximate square root dependence of the Goldstone mass on m_f was demonstrated in ref. [1] and our results confirm this picture. In addition, our data presented in fig. 13 show that f_G varies by very small amounts from random lattice to random lattice and is also independent of m_f having a value ≈ 1.7 in all the cases we have studied.

In field-theoretical models defined in two dimensions, with interactions involving vector currents (as is the case for the Thirring model), the presence of the Goldstone is expected to affect the Green functions. This is because in two dimensions there are no angular momentum quantum numbers and hence transverse vector operators are pseudoscalar operators. Let us consider the trace of the second-order correction to the fermion propagator in the massive Thirring model with the external legs removed. Taking into account the two diagrams contributing to it, we obtain on the random lattice (in units of the coupling constant)

$$\mathrm{Tr}\left(\Delta S_{F2}^{ij}\right) = 8 w_{ik} w_{jl} \left\{ \mathrm{Tr}\left(\gamma_\mu F_{kl} \gamma_\nu F_{ji} \gamma_\mu F_{kl} \gamma_\nu\right) + \mathrm{Tr}\left(\gamma_\mu F_{kl} \gamma_\nu\right) \mathrm{Tr}\left(F_{ji} \gamma_\mu F_{kl} \gamma_\nu\right) \right\}, \quad (4.3)$$

where the traces are over spinor indices (which have been suppressed). With the

definitions of eqs. (3.3a, b) for the interaction, i and k are nearest neighbours, as are j and l and $w_{ik} = \frac{1}{4} l_{ik}\sigma_{ik}$. With the definition of eq. (3.3c), i and k coincide, as do j and l and $w_{ik} = \delta_{ik}\omega_{ik}$. We can rewrite eq. (4.3) as follows

$$\mathrm{Tr}\left(\Delta S_{\mathrm{F2}}^{ij}\right) = 16 w_{ik} w_{jl} \mathrm{Tr}\left(F_{ij}\right) \mathrm{Tr}\left(F_{kl}\gamma_5 F_{lk}\gamma_5\right). \tag{4.4}$$

In the second trace of the right-hand side we recognise the correlation function between pseudoscalar operators $\bar{\Psi}\gamma_5\Psi$ at sites k and l. We thus expect $\mathrm{Tr}(\Delta S_{\mathrm{F2}})$ to be affected by the presence of the Goldstone. In fig. 14 we show the results for $\mathrm{Tr}(\Delta S_{\mathrm{F2}})$ on the same 900-site random lattice used for figs. 11 and 12. Results are presented for definitions (3.3a, b) and for definition (3.3c) for the interaction. They are in good agreement with each other, but they disagree with the continuum curve

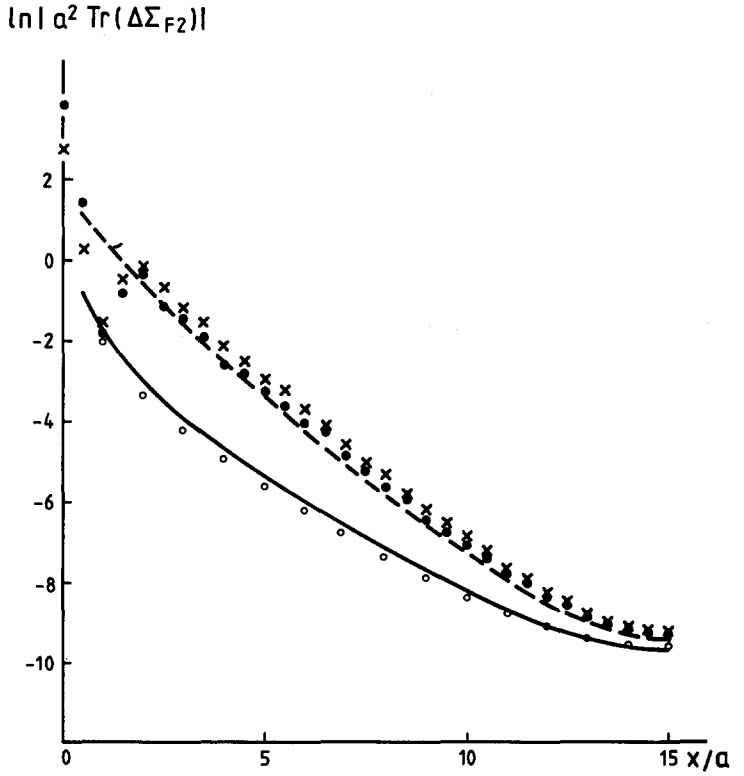

Fig. 14. The trace of the second-order correction to the fermion propagator (with the external legs removed) in the massive Thirring model. The random lattice data are from a 900-site lattice and for $m_t a = 0.16$. × corresponds to the definitions (3.3a, b) for the interaction, while ● corresponds to the definition (3.3c). ○ are data obtained with Wilson fermions on a regular square 900-site lattice. The solid curve is the continuum result, while the dashed curve is obtained by adding to the continuum result the contribution of fig. 15.

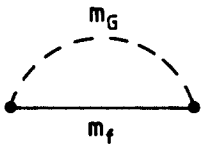

Fig. 15. A diagram representing the contribution of the Goldstone boson to the second-order correction to the fermion propagator in the massive Thirring model (external legs removed).

(solid curve in fig. 14) calculated in a square box the same size as our random lattice. We expect that $\mathrm{Tr}(\Delta\Sigma_{F2})$ consists of the contribution of the primary fermions, which is the same as in the continuum, and of a contribution involving the Goldstone which is represented by the diagram of fig. 15. With the values for m_G and f_G previously obtained we calculate this contribution and add it to the continuum result to obtain the dashed curve in fig. 14 which is in very good agreement with our random lattice results. Note that irrespective of the definition used for the interaction, the right-hand side of eq. (4.4) involves the correlation of pseudoscalar *point* operators $\bar{\Psi}_k\gamma_5\Psi_k$. Hence, it is not always possible to use the trick of point-splitting the pseudoscalar operators in order to eliminate the Goldstone contribution to the results. At this order, point-splitting the interaction by two links will almost decouple the Goldstone. However, at the next order we will get point-like couplings to the Goldstone again, necessitating further splitting of the interaction term, thus making the model unattractive.

5. Discussion

Several models exist in the literature which involve randomness of some sort and seek to remove the doubles at the tree graph level. In particular, the disordered coupling of Weingarten and Velikson [11] has been studied by different approximation techniques. Hernandez and Hill [12] showed that Weingarten and Velikson's Monte Carlo results are in conflict with perturbation theory in the coupling of the fermions to the disordering field. Alessandrini and Krzywicki [13] applied a mean field approximation to calculate the fermion propagator. Alonso and Cortes [14] proposed a simpler model which leads to the same expression for the propagator. Recently, serious doubt has been cast upon the latter two models [15] but the possibility that the Weingarten and Velikson model has a satisfactory continuum limit has not been ruled out; it may avoid doubling at the tree graph level by a chiral-symmetry breaking mechanism similar to that found on the random lattice. In any case, a fuller understanding of the properties of the model is needed at the tree graph level and fully interacting theories are yet to be studied; in particular, to see that non-hermitian effects can be confined to short-distance physics.

By contrast, many properties of fermions on the random lattice now seem well established, at least in two dimensions. At the tree graph level, doubling is evaded through a chiral-symmetry breaking mechanism which gives the doubles large masses. Beyond the tree level, our investigation has revealed properties similar to those of Wilson fermions. Ultraviolet finite graphs have the correct continuum limit. However, our study of the Thirring model suggests that the doubles' contribution to the radiative mass correction behaves like a^{-1}; this does not vanish as $m \to 0$ so that at one loop the chiral symmetry of the primary fermion is broken as well. In practice (e.g. in a Monte Carlo simulation) this creates a fine-tuning problem; a light fermion in the continuum limit is not obtained by simply letting $ma \to 0$.

The fact that the chiral symmetry of the doubles is broken spontaneously, rather than explicitly, at the tree graph level leads to the existence of the Goldstone boson (but see the discussion in the footnote of sect. 1). Although this particle decouples from the theory in the continuum limit, it is relatively light on lattices with a small number of sites; its contribution to the pseudoscalar and vector sector (in two dimensions) has to be taken into account. As we have shown in sect. 4, it appears in loop diagrams as well as tree graphs.

We have not examined gauge theories but our work gives us clues about what to expect. Our results indicate that the Schwinger model, which has no ultraviolet divergent diagrams, can be studied on the random lattice without the introduction of counterterms and should have the correct continuum limit. On a lattice with a finite number of sites we expect the Goldstone contribution to dominate at short distances. Work on the properties of the Schwinger model on the random lattice is in progress. There is enough evidence to suggest that chiral symmetry is spontaneously broken on a four-dimensional random lattice [1, 3] and as a result fermion doubling is evaded at the tree graph level [16]. There is no reason to expect that in four dimensions the divergent diagrams do not receive contributions from the doubles and that problems do not reemerge at the one-loop level. Hence, we expect that a study of QCD on the random lattice would require the introduction and appropriate fine tuning of a mass renormalisation counterterm.

We wish to thank Domenec Espriu, Mark Gross and Paul Rakow for interesting and useful discussions. This work was supported in part by SERC. SJP acknowledges the financial support of the Alexander S. Onassis Public Benefit Foundation.

References

[1] D. Espriu, M. Gross, P.E.L. Rakow and J.F. Wheater, Nucl. Phys. B275 [FS17] (1986) 39
[2] D. Espriu, M. Gross, P.E.L. Rakow and J.F. Wheater, Prog. Theor. Phys. Suppl. 86 (1986) 304
[3] R. Friedberg, T.D. Lee and H.-C. Ren, Prog. Theor. Phys. Suppl. 86 (1986) 322
[4] Y. Pang and H.-C. Ren, Phys. Lett. B172 (1986) 392
[5] N.H. Christ, R. Friedberg and T.D. Lee, Nucl. Phys. B202 (1982) 89
[6] N.H. Christ, R. Friedberg and T.D. Lee, Nucl. Phys. B210 [FS6] (1982) 337

[7] K.G. Wilson, *in* New Phenomena in Subnuclear Physics, ed. A. Zichichi (Plenum, New York, 1977)
[8] L.H. Karsten and J. Smit, Nucl. Phys. B183 (1981) 103
[9] H.S. Sharatchandra, Phys. Rev. D18 (1978) 2042
[10] B. Klaiber, *in* Lectures in Theoretical Physics, ed. A.O. Barut, W. Brittin (Gordon and Breach, New York, 1968)
[11] D. Weingarten and B. Velikson, Nucl. Phys. B270 [FS16] (1986) 10
[12] O. Hernández and B. Hill, Phys. Lett. B178 (1986) 405
[13] V. Alessandrini and A. Krzywicki, Phys. Lett. B177 (1986) 395
[14] J.L. Alonso and J.L. Cortes, Phys. Lett. B187 (1986) 146
[15] M. Gross, P. Lepage and P.E.L. Rakow, On attempts to evade fermion doubling by giving up hermiticity, Cornell University Preprint (1987)
[16] Y. Pang and H.-C. Ren, Columbia Preprint CU-TP-363 (1987)